Physicochemical properties of p-hydroazobenzene: a nonlinear optical crystal

L Guru Prasad[a*] & R Ganapathi Raman[b]

[a]Department of Science & Humanities, M Kumarasamy College of Engineering, Karur – 639 113, India
[b]Department of Physics, Noorul Islam University, Nagercoil, India

Crystal of p-hydroazobenezene was grown and the crystal system is confirmed by analysis the XRD data. The material delineated in monclinic system with the space group of Pbca. FTIR and Raman spectrum analysis have been performed to comprehend the molecular interactions and to learn the vibrational nature of the functional groups in the title compound. Optical, and thermal stability analysis were also been carried out. Exhaustive explorations were conducted on the optical properties of the crystal using both quantum chemical calculations and experimental data.

Keywords: XRD; vibrational analysis; SHG; Hyperpolarisibility; HOMO-LUMO

1 Introduction

Recently, organic nonlinear optical (NLO) materials receive much importance from the researchers because of its frequency conversion property. NLO materials with high frequency conversion in visible and infrared range are requisite for the fabrication of tunable laser[1-3]. Among the available organic NLO materials, photoresponsive azobenzene materials gained much attention[4]**.** This arises as a result of its two isomeric forms: trans- and cis-[5] which hold the advantage and shows high optical nonlinearity. In p-hydroxyazo-compounds, transfer of charges (proton) occurs between the nitrogen and oxygen atoms and these compounds have high tautomeric transformation rate. These charge transfer lead to the formation of long hydrogen bonds[6-7]. Polarizability of these hydrogen bonded systems is high and may show high value of frequency conversion efficiency.

Presence of π-conjugated system in the azo molecule is the added advantage for obtaining high value of frequency conversion efficiency. Apart from the NLO properties, these azobenzene systems also show photo switching properties, which make the aptness of the materials for opto-electronic applications. Hence, in the present investigation we have chosen p-hydroxyazobenzene (PHAB) for crystal growth. Physicochemical properties of PHAB were investigated and results are discussed in this manuscript.

2 Experimental Details

PHAB have been prepared as crystals using solution evaporation technique. Commercially obtainable p-hydroxyazobenzene (PHAB) was used for crystallization process. The saturated solution of PHAB was prepared in ethanol and in order to the unstaturated materials and impurities the prepared solution was filtered out. This filtered out solution was covered by punctured polythene sheet and kept for evaporation of solvent. After 2 weeks with of period PHAB crystal was obtained.

3 Results and Discussions.

3.1 Crystallography studies

XRD of PHAB was recorded using powder sample of PHAB and data obtained from Riche Seifert SH-37/80 diffractometer. CuKα radiation with 1.5405 Å wavelength was used for the diffraction.

Recorded XRD pattern of PHAB was indexed using XRDA software and is shown in Fig. 1. From the analysis, it is confirmed that the grown material are in monoclinic crystal system which is agreed with previously report values[8]**.** The spiky peaks indicate the purity of the grown PHAB. Obtained unit cell values are tabularized in Table. 1.

3.2 Vibrational analysis

FTIR and FTR a man spectrum of PHAB were documented in the wave number range of 400-4000 cm^{-1} and 40-4000 cm^{-1} using Brucker IF S66V and Brucker RFS 27 Spectrometer respectively.
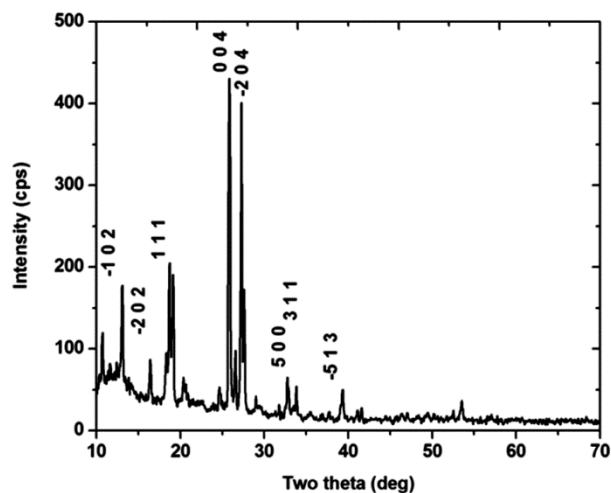
———————
Corresponding author (E-mail: guruprasadl.snh@mkce.ac.in)

Fig.1   XRD pattern of PHAB
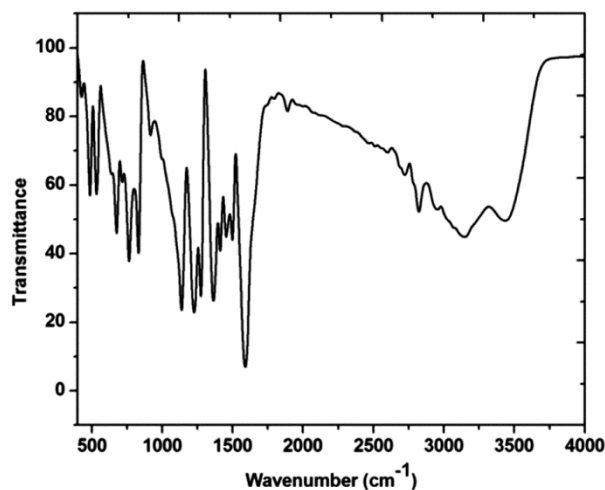
Fig.2   FTIR spectrum of PHAB

Table 1 — Crystallographic data of Ag_2S

	Lattice Parameters	
	Reported (E.B. Shamuratov et al., 1991)	Present Investigation
a (Å)	13.753	13.181
b (Å)	5.619	5.62884
c (Å)	14.023	13.94195
β	98.31	102.56
Cell Volume ($Å^3$)	1072.3	1009.68

Documented FTIR spectrum and FTR a man are given in Figs. (2-3). Identified peaks were assigned to its vibrational groups and given in Table. 2.

Hydroxyl groups

OH group vibrations are sensitive to the environment; in general free OH group can be observed in the region of 3500-3700 cm^{-1}. If the system has any inter, intra molecular hydrogen bond means the frequency of the hydroxyl groups gets shifted to lower wave number region. In the current investigation, the OH stretching vibration is traced at 3435 cm^{-1} and it confirms the presence of inter molecular hydrogen bonding[9]. The intensity of the observed OH band is higher than the free OH band and peak is quite broader. This confirms the hydroxyl group present in the title molecule actively involved in intermolecular hydrogen bond formation[9-10]. Presence of hydrogen bonding and due to the steric effect, the location of O–H stretching band has shifted to higher wavenumber region. Normally, phenyl ring mode gives a very strong band in IR spectra. Band at 1590 cm^{-1} in FTIR and 1591 cm^{-1} in FTR a man
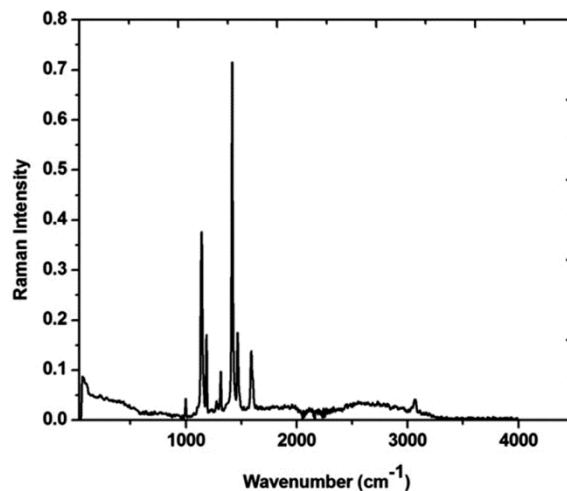

Fig.3   FTRaman spectrum of PHAB

Table 2 — Vibrational assignments of PHAB

Observed Vibrational bands (cm-1)	Assignments
3435	OH stretching
3146	CH stretching
3069	CH stretching
1590	Ring mode vibration, CO stretching
1455	Ring mode vibration, CO stretching
1413	CO stretching, aromatic ring vibration
1364	CN stretching
1315	CN stretching
533	CN stretching

confirms the presence of phenyl ring mode vibrations in the grown crystal. The strong intensity of 1590 cm^{-1} band in IR spectra could be interpreted to be the intra molecular charge transfer.

Azo group

Since azo group being non-polar in nature, it is very difficult to identify its vibrations in the IR spectra. Further, the overlapping of aromatic vibration bands with the azo group makes more difficult to identify the azo vibrations in IR spectra. Nevertheless, the azo groups give strong intensity bands in Raman spectra. Trans- form of aromatic compounds traces peak at 1465-1380 cm⁻¹ and the cis – form records peak near to 1510 cm⁻¹. Unsymmertical P-substituted azo-benzene shows a peak near to 1430 cm⁻¹ but in the current analysis this band get relocated to lower wave number region and observed at 1413 cm⁻¹. This shift arises because of the presence of hydroxyl group in the para position. In IR spectra, a band observed at 533 cm⁻¹ due to CN stretching and C-N=N deformation vibrations.

CN vibrations

Stretching of CN bond shows medium to weak absorption bands near to 1020-1250 cm⁻¹. Generally these vibrations are coupled with the stretching of adjacent bonds hence the force constant of CN bond gets increase and it can be observed at the higher wavenumber region[11]. In the title molecule the peak noticed at 1364 cm⁻¹ in FTIR and at 1315 cm⁻¹ in FTR a man is consigned to CN stretching vibration. The shift in observed band arises due to the neighboring groups, conjugation effects, hydrogen bonding and molecular tautomersim.

CH vibrations

Two non degenerate and two degenerate modes of vibrations can generally observed in the benzene derivates. In p-substituted benezene, four of these CH stretching vibrations show peaks in the region of 3000-3100 cm⁻¹. In the present investigation, the peaks observed at 3146 cm⁻¹ in FTIR and 3069 cm-1 in FTR a man are assigned to CH stretching vibrations. Owing to the inductive effect, these bands have been noticed at higher wavenumber side. In the substituted benzene, the in-plane and out-plane CH vibrations come into sight between 1000-1300 cm⁻¹ and between 750-1000 cm⁻¹ correspondingly[12].

Carbonyl group vibrations

The characteristic vibration of carbonyl group can be observed in the vibrational spectra. The intensity of carbonyl vibration peak depends on the quantity of hydrogen bonds in the molecule. For the title compound, strong and sharp intense peaks are observed in both Raman and FTIR at 1413, 1455 and 1590 cm⁻¹ is arises due to C–O stretching vibrations. This intensification of Raman and IR line confirms the presence of hydrogen bonds in the grown system.

3.3 Optical analysis

The Optical characteristics of the grown crystal PHAB (Fig. 4) was studied with the wavelength range of 190nm-1100nm by SCHIMADZU UV-VIS-NIR spectrophotometer 4-phenylazophenol has excellent lucidity in the visible region and its maximum absorption was at 340 nm. The band at 230 nm and 340 nm were connected to the π to π* transition of the phenyl groups and hydrazone form.

Photoluminescence study for PHAB was carried out using Shimadzu pectrofluorophotomete and the recoded emission spectrum is given in Fig. 5.
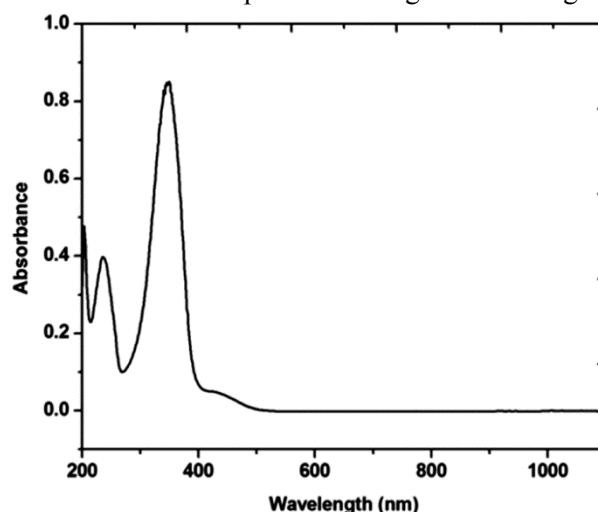

Fig. 4   UV-VIS-NIR spectrum of PHAB
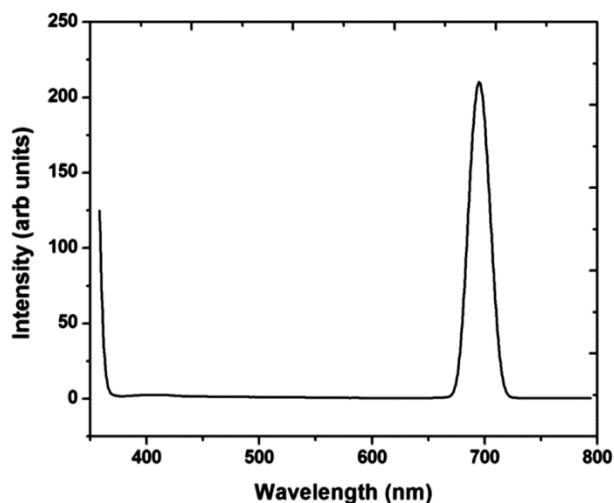

Fig. 5   Photoluminescence spectrum of PHAB

Excitation was carried out for the prepared sample at 250 nm. The PHAB crystal emits the light of wavelength 700 nm in nominal red edge of visible spectrum.

Polarizability and Hyperpolarizability studies

Polarizability and first order hyperpolarizability (β) values of PHAB were simulated using Gaussian 09 package[13] and tabulated in Table. 3. Optimization of molecule was carried at B3LYP/6-31 g and hyperpolarizability calculation was done with HF/6-31g level. Large value was found in the direction of β_{xxx}. It is visible that the title molecule has large value of first order hyperpolarizability (6.0108×10^{-30} esu) and it suggests the suitability of the compound for NLO process[14].

HOMO- LUMO analysis

Orbital analysis helps to analysis the charge

Table 3 — Hyperpolarizability values of PHAB

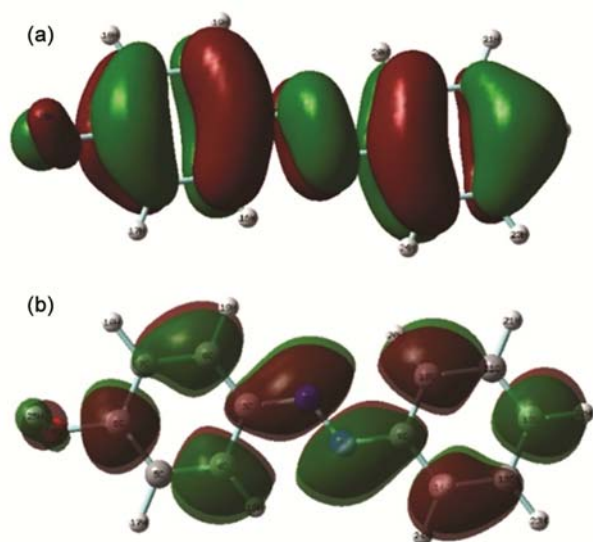| Direction	Hyperpolarizability ($\times 10^{-30}$ esu)
β_{xxx}	8.15968
β_{xxy}	0.455
β_{xyy}	0.6470
β_{yyy}	0.1783
β_{xxz}	0.0009
β_{xyz}	0
β_{yyz}	0
β_{xzz}	0.0228
β_{yzz}	0
β_{zzz}	0
β_{tot}	6.0108

Fig. 6   (a) HOMO and (b) LUMO diagram of PHAB

transport nature of the molecule[15-16]. The HOMO-LUMO energy gap of PHAB is 0.3459 a.u. The small value of energy gap reveals the chance of charge transfer inside the NTSAD. Obtained HOMO-LUMO diagram is shown in Fig. 6.

Due to the existence of weak bond in the grown crystal, larger hyperpolarizability value and low HOMO-LUMO energy gap occurs[17]. These low values of HOMO-LUMO energy gap and charge transfer nature are the added advantages for the SHG.

Powder SHG Measurement

Kurtz–Perry powder technique is widely used to confirm second harmonic generation of the materials. Experiments were performed with personalized s etup of Kurtz and Perry[18]. Initially PHAB sample was powdered and filled in the micro capillary tube and which was illuminated with the wavelength of 1064nm laser light. SHG emission from the samples was confirmed and the relative conversion of SHG efficiency is about 0.5 times of standard KDP.

3.4 Thermal analysis

Thermal stability of the PHAB compound was analyzed using PerkinElmer Diamond instrument in a nitrogen atmosphere at a heating rate of 10 °C min^{-1} and carried out in a temperature range of 200-1200 °C, is picturized in Fig. 7. It is noticed that the weight loss occurs at 269 °C and underneath this there no considerable weight loss. This gives a proof that the unit cell of PHAB has no inclusion of water molecule. Two endothermic peaks were observed in DSC at 159 ºC and at 655 ºC. First spiky peak arises due to
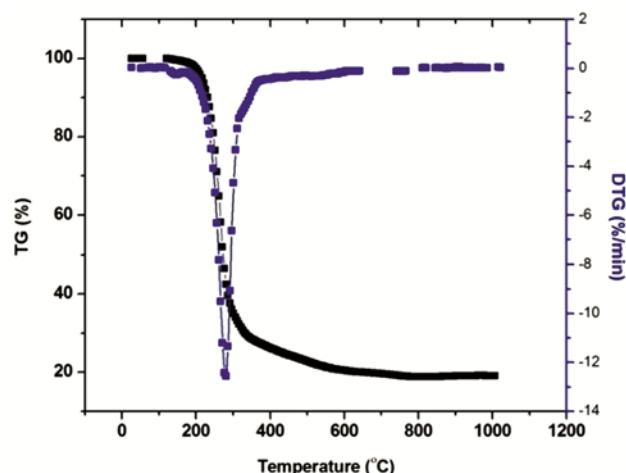

Fig.7   TG-DTA of PHAB

the melting point of PHAB crystals. The second peak observed at 655 ºC is the counterpart of weight loss. Presence of isothermic transition is confirmed by the non evidence of endothermic or exothermic peak before 159.7 ºC.

4 Conclusions

PHAB crystals were grown by solvent evaporation technique. Crystal system of the grown crystal was confirmed by analyzing the XRD peaks. Vibrational groups and its vibrational frequencies were identified in both FTIR and FTRaman spectrum. Thermal stability of PHAB was also analyzed. NLO properties of the PHAB were confirmed both computationally and experimentally.

References

1 Boomadevi S, Mittal H P & Dhansekan R, *J Cryst Growth*, 261 (2004) 55.
2 Prasad L G, Krishnakumar V & Nagalakshmi R, *Spectrochim Acta A*, 110 (2013) 377.
3 Prasad L G, Krishnakumar V, Nagalakshmi R & Manohar S, *Mater Chem Phys*, 128 (2011) 90.
4 Hamon F, Djedaini-Pilard F, Barbot F & Len C, *Tetrahedron*, 65 (2009) 10105.
5 Gayathri C & Ramalingam A, *Spectrochim Acta A*, 69 (2008) 96.
6 Qi S, Yang X, Lu R, Chen K, Zhang C, Tian J, Xu J & Wu Q, *J Modern Opt*, 51 (2004) 1671.
7 Kondrashev Y D, *J Struct Chem*, 15 (1974) 574.
8 Shamuratov E B, Batsanov A S, Struchkov Y T, Shukurov A, Makhsumov A G & Saabirov V K, *Zhurnal Struklurnoi Khimii*, 32 (1991) 146.
9 Karabacak M & Kurt M, *J Mol Struct*, 919 (2009) 215.
10 Krishnakumar V & Mathammal R, *J Raman Spectrosc*, 40 (2009) 1599.
11 Krishnakumar V, Manohar S & Nagalakshmi R, *Spectrochim Acta A*, 71 (2008) 110.
12 Alpert N L, Keiser W E & Szymanski H A, Theory and Practice of Infrared Spectroscopy, Plenum/Rosetta Ed, 1973.
13 Gaussian 09, Revision A02, Frisch M J, Trucks G W, Schlegel H B, Scuseria G E, Robb M A, Cheeseman J R, Scalmani G, Barone V, Petersson G A, Nakatsuji H, Li X, Caricato M, Marenich A, Bloino J, Janesko B G, Gomperts R, Mennucci B, Hratchian H P, Ortiz J V, Izmaylov A F, Sonnenberg J L, Williams-Young D, Ding F, Lipparini F, Egidi F, Goings J, Peng B, Petrone A, Henderson T, Ranasinghe D, Zakrzewski V G, Gao J, Rega N, Zheng G, Liang W, Hada M, Ehara M, Toyota K, Fukuda R, Hasegawa J, Ishida M, Nakajima T, Honda Y, Kitao O, Nakai H, Vreven T, Throssell K, Montgomery J A, Peralta J E, Ogliaro F, Bearpark M, Heyd J J, Brothers E, Kudin K N, Staroverov V N, Keith T, Kobayashi R, Normand J, Raghavachari K, Rendell A, Burant J C, Iyengar S S, Tomasi J, Cossi M, Millam J M, Klene M, Adamo C, Cammi R, Ochterski J W, Martin R L, Morokuma K, Farkas O, Foresman J B & Fox D J, Gaussian, Inc, Wallingford CT, 2016.
14 Avcı D, Cömert H & Atalay Y, *J Mol Model*, 14 (2008) 161.
15 Fukui K, *Science*, 218 (1982) 9.
16 Tamer O, Avcı D & Atalay Y, *Spectrochim Acta A*, 117 (2014) 78.
17 Jothy V B, Vijaykumar T, Jayakumar V S, Udayalekshmi K, Ramamoorthy K & Joe I H, *J Raman Spectrosc*, 38 (2007) 1148.
18 Kurtz S K & Perry TT, *J Appl Phys*, 39 (1968) 3798.